JOURNAL OF COMPUTATIONAL PHYSICS **132,** 167–174 (1997)
ARTICLE NO. CP965635

Compact Finite Difference Method for Calculating Magnetic Field Components of Cyclotrons[1]

Dong-o Jeon

National Superconducting Cyclotron Laboratory, Michigan State University, East Lansing, Michigan 48824-1321

Received May 30, 1995; revised September 4, 1996

The compact finite difference method was developed for calculating the off median plane magnetic field components of cyclotrons when only the measured midplane field data are available. It has been shown that the proposed compact finite difference differentiators are better than the finite difference differentiators previously reported by the author. The proposed compact finite difference method was tested by comparing the frequency response, by applying to an analytical magnetic field, and by applying to measured magnetic field data of the K1200 superconducting cyclotron at the National Superconducting Cyclotron Laboratory. It should be pointed out that this improvement was obtained at the expense of more complicated machinery of mathematics, namely solving matrix problems.

1. INTRODUCTION

In most cases with cyclotrons, magnetic field only on the median plane is measured due to narrow gaps of magnets and these midplane field data are utilized for various beam dynamics computations. Median plane field data are sufficient for computing linear properties of beams, while off median plane field components are necessary for calculating nonlinear properties. Using a fourth-order vector potential and the measured midplane field data, and assuming midplane field symmetry, the magnetic field components up to z^4 [1] are given by

$$B_z = B(r, \theta) - \frac{z^2}{2!}\nabla_2^2 B(r, \theta) + \frac{z^4}{4!}\nabla_2^4 B(r, \theta), \tag{1}$$

$$B_r = \frac{\partial}{\partial r} C(r, \theta, z), \tag{2}$$

$$B_\theta = \frac{\partial}{r\partial\theta} C(r, \theta, z), \tag{3}$$

where B_z, B_r, and B_θ are magnetic field components in cylindrical polar coordinates and where

$$C(r, \theta, z) = zB(r, \theta) - \frac{z^3}{3!}\nabla_2^2 B(r, \theta)$$

and

$$B(r, \theta) = B_z(r, \theta, z = 0).$$

Note that $\nabla_2^2 = \partial^2/\partial r^2 + \partial/r\partial r + \partial^2/r^2\partial\theta$ is the two-dimensional Laplacian operator in cylindrical polar coordinates and that no source is assumed to exit on the median plane. In addition, this representation satisfies $\nabla \cdot \mathbf{B} = 0$.

Gordon and Taivassalo [1, 2] evaluated the coefficients of expansion series using the second-order central difference scheme,

$$f_i' = (f_{i+1} - f_{i-1})/2\Delta \tag{4}$$

$$f_i'' = (f_{i+2} + f_{i-2} - 2f_i)/4\Delta^2, \tag{5}$$

where $f_i = f(x_i)$ and Δ is the step size of the mesh $\{x_i\}$. These schemes presented difficulties both in accuracy and maximum order of expansion due to amplified noise produced by taking derivatives. The two-dimensional Laplacian operator ∇_2^2 should be applied successively to get higher order coefficients of the Taylor series. Differentiation amplifies the high frequency signals considerably which contain noise from various sources. If an effective suppression of the high frequency signals is not achieved, successive differentiation will soon destroy the significance of the obtained data. Differentiators should also evaluate accurately the derivatives of signals over a sufficiently wide range of low frequency.

Because the measured data of $B(r, \theta)$ contain some error or noise presumably in the rapidly varying Fourier components, a specifically designed low-pass filter was employed to suppress the effects of these rapidly varying components when taking derivatives. As is pointed out in the introduction of the previous paper [3], there are two possible ways to compute derivatives of measured midplane magnetic field data numerically. One way to do so

[1] Work supported by the National Science Foundation under Grant Phy. 92-14992.

0021-9991/97 $25.00

is to process a magnetic field using a certain low-pass filter to remove the high frequency components before taking any derivatives and to apply differentiators successively to the processed field data to the desired order. This is relatively simple and straightforward. The other way is to use a combination of a low-pass filter and differentiators (called ''intermediate differentiators'' in Section 2) whenever differentiation is performed. Although it is rather complicated, we decided to take the latter in order to maintain consistency with the linear orbit codes that use only the measured magnetic field data on the median plane without any filtering.

Compact finite difference schemes were used both for the low-pass filter and the intermediate differentiators to enhance the characteristics of the slowly varying Fourier components of derivatives in comparison with the finite difference method that was presented by the author [3] for solving this problem. A lot of work on compact finite difference schemes has been done [4–6]. Especially, Lele [7] did recent work on compact finite difference schemes and the proposed compact finite difference method was motivated by his work.

In Section 2 are presented the proposed first and second differentiators for the one-dimensional data array which are a combination of a low-pass filter and intermediate differentiators. In Section 3 are given the proposed first and second differentiators for the two-dimensional data array which are a combination of primary and secondary low-pass filters and intermediate differentiators. In Section 4 we applied the proposed differentiators for the two-dimensional data array to the magnetic field produced by two infinite saturated iron bars. The significance of this magnetic field is that this is the only case where we have analytical forms for the field. In Section 5 is given the result of application to the measured magnetic field data of K1200 superconducting cyclotron at the National Superconducting Cyclotron Laboratory at Michigan State University. And finally, a conclusion is given in Section 6.

2. FIRST AND SECOND DIFFERENTIATORS IN ONE-DIMENSION

As was noted above, the proposed differentiators are combinations of a low-pass filter and ''intermediate differentiators,'' which can be schematically depicted as

Data to be processed
⇓
Low-pass filter
⇓
Intermediate first or second differentiator
⇓
Data of derivatives.

The employed low-pass filter takes on the form

$$\begin{aligned}&\beta F_{i-2} + \alpha F_{i-1} + F_i + \alpha F_{i+1} + \beta F_{i+2}\\ &\quad = af_i + \frac{b}{2}(f_{i+1} + f_{i-1}) + \frac{c}{2}(f_{i+2} + f_{i-2}) + \frac{d}{2}(f_{i+3} + f_{i-3}),\end{aligned} \tag{6}$$

where F_i is the filtered values of f_i at x_i and α, β, a, b, c, and d are properly chosen constants. The reason why these schemes are called ''compact'' is that either α or β is nonzero. If all of them are zero, these schemes are reduced to finite difference schemes.

The frequency response of this filter is

$$H^{(F)}(\omega) = \frac{a + b\cos\omega + c\cos 2\omega + d\cos 3\omega}{1 + 2\alpha\cos\omega + 2\beta\cos 2\omega}. \tag{7}$$

When the following constraints are applied

$$H^{(F)}(\pi) = 0, \qquad \text{and} \qquad \frac{d^2H^{(F)}}{d\omega^2}(\pi) = 0, \tag{8}$$

in addition to formal fourth-order accuracy, a two-parameter family of schemes of derivatives is obtained that is defined by

$$\begin{aligned}a &= \frac{1}{4}(2 + 3\alpha), \qquad b = \frac{1}{16}(9 + 16\alpha + 10\beta),\\ c &= \frac{1}{4}(\alpha + 4\beta), \qquad d = \frac{1}{16}(6\beta - 1),\end{aligned} \tag{9}$$

with a truncation error $(1/16)(3 - 2\alpha - 10\beta)\,\Delta^4 f^{(4)}$ where Δ is the step size. Imposing the sixth-order constraint to the above, we get

$$\begin{aligned}\beta &= \frac{3 - 2\alpha}{10}, \qquad a = \frac{2 + 3\alpha}{4}, \qquad b = \frac{6 + 7\alpha}{8},\\ c &= \frac{6 + \alpha}{20}, \qquad d = \frac{2 - 3\alpha}{40}.\end{aligned} \tag{10}$$

Finally, when the constraint $(d^4H^{(F)}/d\omega^4)(\pi) = 0$ is imposed, a scheme with the coefficients

$$\begin{aligned}\alpha &= 0, \qquad \beta = \frac{3}{10}, \qquad a = \frac{1}{2},\\ b &= \frac{3}{4}, \qquad c = \frac{3}{10}, \qquad d = \frac{1}{20}\end{aligned} \tag{11}$$

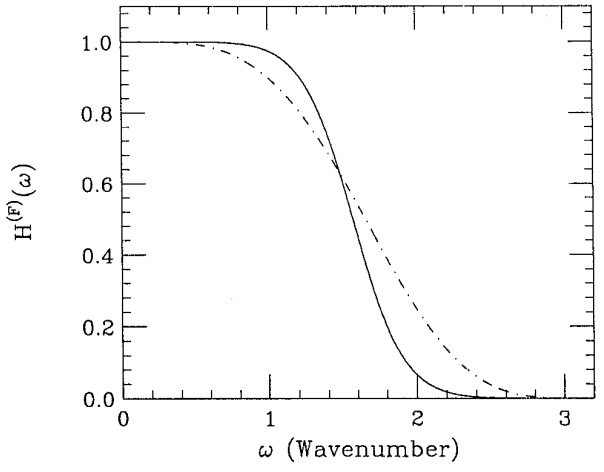

FIG. 1. Plot of the frequency response of the low-pass filter (solid line) used for the proposed differentiator together with that of the low-pass filter used for the finite difference differentiator [3] (dot-dash line). The proposed filter has a wider band of passage, stronger suppression of high ω components, and sharper cutoff frequency than the filter used for the finite difference differentiator.

is obtained. The resultant frequency response is

$$H^{(F)}(\omega) = \frac{1/2 + (3/4)\cos\omega + (3/10)\cos 2\omega + (1/20)\cos 3\omega}{1 + (3/5)\cos 2\omega}, \quad (12)$$

and is depicted in Fig. 1. This is characterized by a relatively sharply defined cutoff frequency, enhanced low frequency behavior, and a strong high frequency suppression.

The intermediate first differentiator used for the proposed scheme takes on the form

$$\alpha f'_{i-1} + f'_i + \alpha f'_{i+1} = a\frac{f_{i+1} - f_{i-1}}{2\Delta} + b\frac{f_{i+2} - f_{i-2}}{4\Delta}, \quad (13)$$

where f'_i is the approximate value of the first derivative at x_i. With the following choices of parameters, a family of tridiagonal schemes with a formal fourth-order truncation error $(4/5!)(3\alpha - 1)\,\Delta^4 f^{(5)}$ is obtained:

$$a = \frac{2}{3}(\alpha + 2), \qquad b = \frac{1}{3}(4\alpha - 1). \quad (14)$$

With a choice of $\alpha = 1/3$, the scheme becomes formally sixth-order accurate with a truncation error $(4/7!)\,\Delta^6 f^{(7)}$ and the coefficients are

$$\alpha = \frac{1}{3}, \qquad a = \frac{14}{9}, \qquad b = \frac{1}{9}. \quad (15)$$

The corresponding frequency response of this intermediate first differentiator is

$$H_0^{(1)}(\omega) = i\frac{(14/9)\sin\omega + (1/18)\sin 2\omega}{1 + (2/3)\cos\omega}. \quad (16)$$

The intermediate second differentiator takes on the form

$$\alpha f''_{i-1} + f''_i + \alpha f''_{i+1} = a\frac{f_{i+1} + f_{i-1} - 2f_i}{\Delta^2} + b\frac{f_{i+2} + f_{i-2} - 2f_i}{4\Delta^2}, \quad (17)$$

where f''_i is the approximate value of the second derivative at x_i. With the following choices of parameters, a family of tridiagonal schemes with a formal fourth-order truncation error $(-4/6!)(11\alpha - 2)\,\Delta^4 f^{(6)}$ is obtained:

$$a = \frac{4}{3}(1 - \alpha), \qquad b = \frac{1}{3}(10\alpha - 1). \quad (18)$$

With $\alpha = 2/11$, a tridiagonal scheme with a formal sixth-order accuracy is obtained:

$$\alpha = \frac{2}{11}, \qquad a = \frac{12}{11}, \qquad b = \frac{3}{11}. \quad (19)$$

The corresponding frequency response is

$$H_0^{(2)}(\omega) = \frac{(24/11)(\cos\omega - 1) + (3/22)(\cos 2\omega - 1)}{1 + (4/11)\cos\omega}. \quad (20)$$

The frequency response of the proposed first (second) differentiator, $H^{(1)}(\omega)(H^{(2)}(\omega))$, is given as a product of the frequency response of the low-pass filter and that of the intermediate first (second) differentiator:

$$H^{(1)}(\omega) = H_0^{(1)}(\omega)H^{(F)}(\omega), \quad (21)$$

$$H^{(2)}(\omega) = H_0^{(2)}(\omega)H^{(F)}(\omega). \quad (22)$$

In Fig. 2 (Fig. 4) is depicted the frequency response of the proposed first (second) differentiator for $0 \le \omega \le \pi$ together with that of the first (second) finite difference differentiator in [3] and that of the scheme in Eq. 23 (Eq. 24) for comparison:

$$f'_i = \frac{1}{2\Delta}(f_{i+1} - f_{i-1}), \quad (23)$$

$$f''_i = \frac{1}{4\Delta^2}(f_{i+2} + f_{i-2} - 2f_i). \quad (24)$$

Here, $\omega = 1.05$ corresponds to the 60th azimuthal harmonic

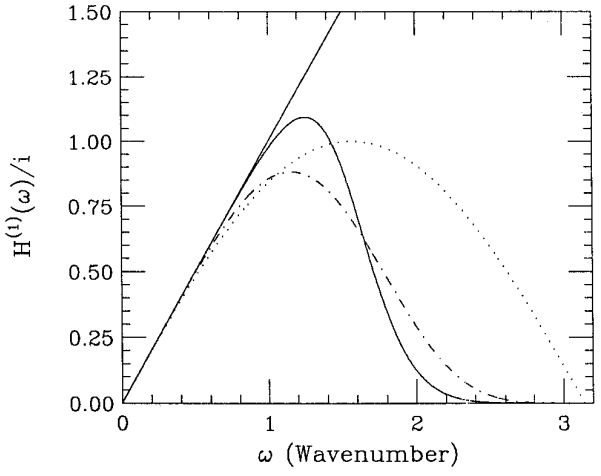

FIG. 2. Plots of the frequency response of several first differentiators divided by i: mathematical differentiation (straight solid line), the proposed compact finite difference differentiator (solid line), the finite difference differentiator [3] (dot-dash line), and the scheme in Eq. (23) (dotted line). The compact finite difference differentiator is accurate over wider range of low ω and suppresses high ω components more effectively than the finite difference differentiator and the scheme in Eq. (23).

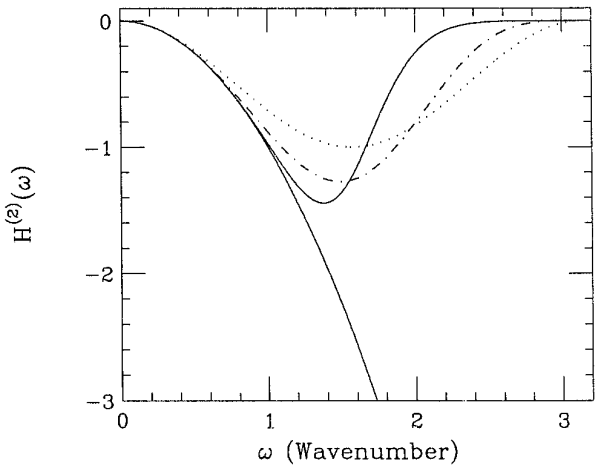

FIG. 4. Plots of the frequency response of several second differentiators: mathematical differentiation (quadratic solid line), the proposed compact finite difference differentiator (solid line), the finite difference differentiator [3] (dot-dash line), and the scheme in Eq. 24 (dotted line). The compact finite difference differentiator is accurate over a wider range of low ω and suppresses high ω components more effectively than the finite difference differentiator and the scheme in Eq. (24).

for a 360° field data with $\Delta\theta = 1°$ and the fractional error in the frequency response of the first (second) differentiator is 3.7% (4.1%), which is quite small. When the magnetic field of the K1200 superconducting cyclotron was Fourier analyzed, it was found that the amplitude above the 40th harmonic is already negligible. So the proposed differentiators are sufficient for handling the field data of the K1200 cyclotron.

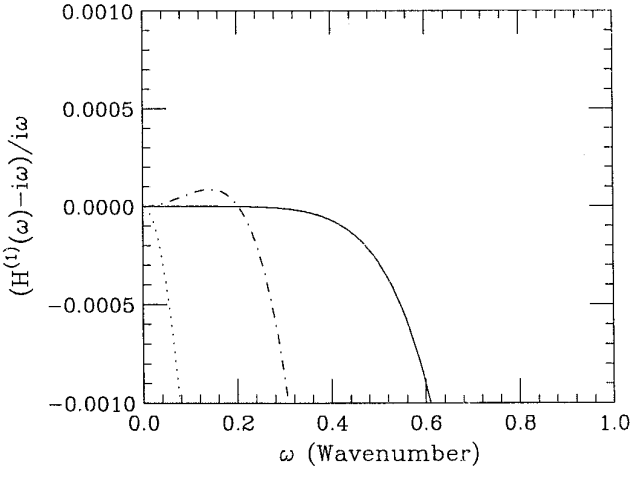

FIG. 3. Plots of the fractional error in the frequency response of the first differentiators in Fig. 2: the compact finite difference differentiator (solid line), the finite difference differentiator [3] (dot-dash line), and the scheme in Eq. (23) (dotted line). Clearly, the proposed compact finite difference differentiator is accurate over a wider range of low ω than the other two differentiators.

In Fig. 3 (Fig. 5) is depicted the fractional error in the frequency response of the proposed first (second) differentiator from that of mathematical first (second) differentiation for $0 \le \omega \le 1$. Figure 3 (Fig. 5) also shows the curves of fractional error in the frequency response of the finite difference differentiator [3] and the first (second) differentiator in Eq. 23 (Eq. 24). Judging from Figs. 2 and 4 together with Figs. 3 and 5, the proposed first (second) compact finite difference differentiator performs accurately over wider range of low ω and suppresses high ω components more effectively than the first (second) finite difference differentiator presented in [3]. Indeed, the proposed compact finite difference differentiators are improved compared with the finite difference differentiators [3]. Of course, this was obtained at the expense of more complicated machinery of mathematics, namely solving matrix problems.

3. FIRST AND SECOND DIFFERENTIATORS IN TWO-DIMENSION

The proposed first and second differentiators in two-dimension are identical to those in one-dimension except that they are accompanied by a "secondary low-pass filter" in $y(x)$ when taking partial derivatives with respect to $x(y)$. The same low-pass filter is used for both primary and secondary low-pass filters. The following diagram shows a schematic flow diagram of the proposed differentiators:

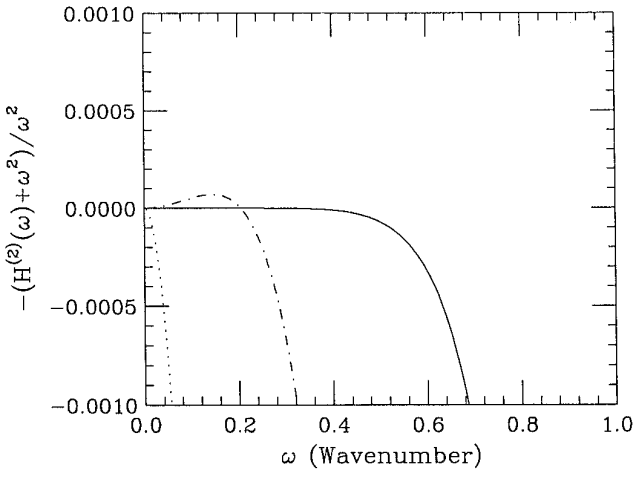

FIG. 5. Plots of the fractional error in the frequency response of the second differentiators in Fig. 4: the compact finite difference differentiator (solid line), the finite difference differentiator [3] (dot-dash line), and the scheme in Eq. (24) (dotted line). Clearly the proposed compact finite difference differentiator is accurate over a wider range of low ω than the other two differentiators.

Data to be processed
⇓
Primary low-pass filter
⇓
Intermediate first or second differentiator
⇓
Secondary low-pass filter
⇓
Data of derivatives.

This secondary filter provides some benefits when dealing with data that are prone to error (or noise), as is pointed out in [3] (in [3], this is called a ''vertical filter''). If data do not contain any error (or noise) including truncation error, the secondary filter is useless and only adds unnecessary complexity.

The frequency response of the proposed first partial differentiator with respect to x is

$$H_x^{(1)}(\omega_x, \omega_y) = H^{(F)}(\omega_y) H_0^{(1)}(\omega_x) H^{(F)}(\omega_x), \qquad (25)$$

and that of the proposed second partial differentiator with respect to x is

$$H_x^{(2)}(\omega_x, \omega_y) = H^{(F)}(\omega_y) H_0^{(2)}(\omega_x) H^{(F)}(\omega_x), \qquad (26)$$

4. APPLICATION TO THE MAGNETIC FIELD PRODUCED BY MAGNETIZED IRON BARS

Two long saturated iron bars were considered with the geometry $-2 \le x \le 2$, $-2 \le y \le 2$, and $1 \le z$ for one iron bar and $-2 \le x \le 2$, $-2 \le y \le 2$, and $z \le -1$ for the other. These bars are uniformly magnetized in the $+z$ direction. Let us define $x_1 = -2$, $x_2 = 2$, $y_1 = -2$, and $y_2 = 2$. The magnetic field due to the two sheets of surface charge [1, 8] is analytically given by

$$B_z(x, y, z) = \frac{B_s}{4\pi} \sum_{i,j} (-1)^{i+j} \left[\arctan \frac{X_i Y_j}{Z_+ R_+} + \arctan \frac{X_i Y_j}{Z_- R_-} \right], \qquad (27)$$

where $i, j = 1, 2$, and $B_s = 21.4$ kG [1],

$$X_i = x - x_i,$$
$$Y_j = y - y_j,$$
$$Z_+ = 1 + z,$$
$$Z_- = 1 - z,$$
$$R_\pm = (X_i^2 + Y_j^2 + Z_\pm^2)^{1/2}.$$

$B_z(x, y, z)$ is Taylor expanded around $z = 0$ as in Eq. (1) with

$$B(x, y) = B_z(x, y, z = 0). \qquad (28)$$

The program ''Mathematica'' was used to obtain the analytical expressions of various derivatives such as $\nabla_2^2 B$, $\nabla_2^4 B$, and $\nabla_2^6 B$ with $\nabla_2^2 = \partial^2/\partial x^2 + \partial^2/\partial y^2$. Using these analytically obtained terms evaluated at $z = 0.5$ as a reference, accuracy of the proposed compact finite difference scheme together with the other two schemes was measured in terms of *rms* error from the values of the corresponding terms that are analytically obtained. The other two schemes are the finite difference scheme presented in [3], and the scheme in Eq. (24). In Table I, the values of *rms* error in the various terms obtained by using the three different schemes are listed, where ''CFD scheme'' stands for the proposed compact finite difference scheme in this paper and ''FD scheme'' the finite difference scheme presented in [3]. As an example, the map of the error in the values of $\nabla_2^2 B \times 0.5^2/2!$ obtained by using the CFD (FD) scheme is depicted at bottom (top) in Fig. 6 over the range $-4 \le x \le 4$ and

TABLE I

rms Error in Units of G

Term for comparison	CFD scheme	FD scheme	Scheme in Eq. (24)
$\nabla_2^2 B \times 0.5^2/2!$	2.55×10^{-2}	3.60×10^{-1}	5.34
$\nabla_2^4 B \times 0.5^4/4!$	8.26×10^{-2}	5.98×10^{-1}	3.79
$\nabla_2^6 B \times 0.5^6/6!$	1.12×10^{-1}	4.54×10^{-1}	1.59

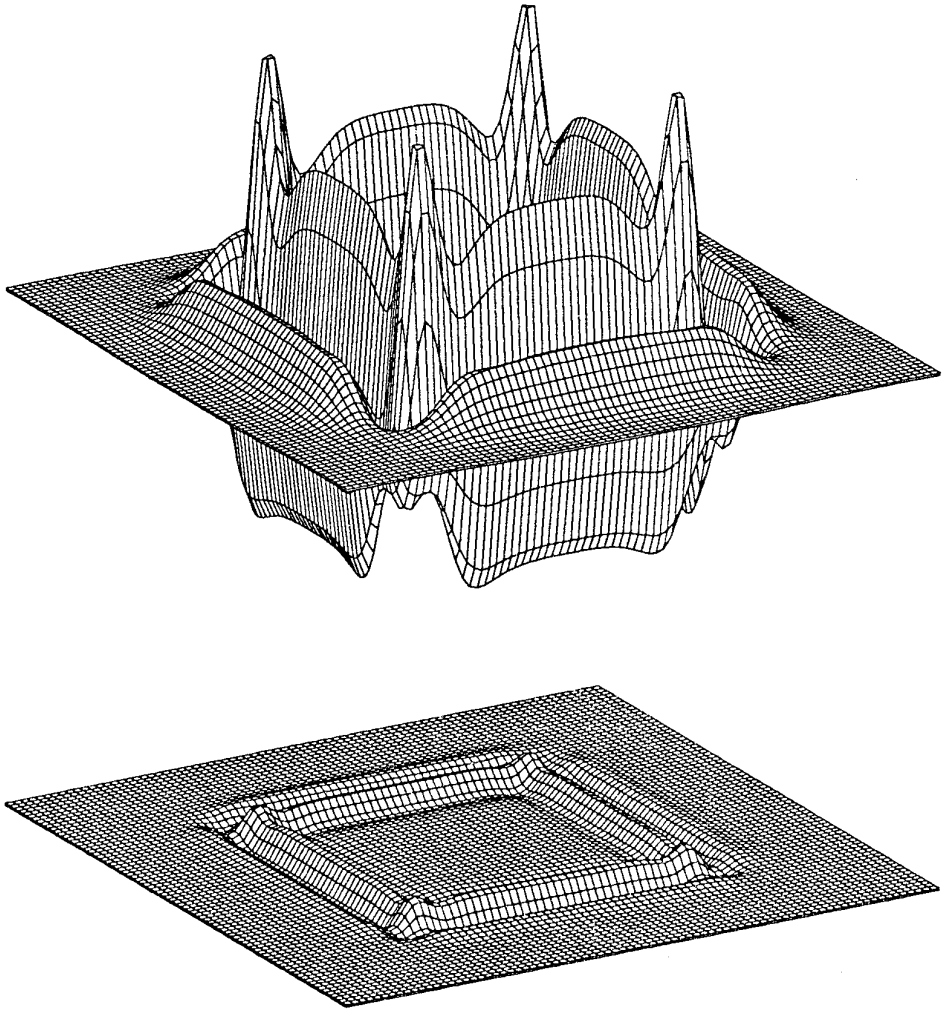

FIG. 6. Plots of the error in $\nabla_2^2 B \times 0.5^2/2!$ obtained by using two different differentiators over $-4 \le x \le 4$ and $-4 \le y \le 4$ with $\Delta x = \Delta y = 0.1$. The bottom map shows the error produced by the proposed compact finite difference differentiator, while the top map shows the error produced by the finite difference differentiator in [3]. The maximum value of the bottom (top) map is 0.123 G (1.49 G) and the minimum value of the bottom (top) map is −0.085 G (−1.09 G). Both maps are depicted to the same scale. It should be pointed out that these errors are very small compared with the maximum (minimum) value of $\Delta_2^2 B \times 0.5^2/2!$ which is 447 G (−948 G).

$-4 \le y \le 4$. The maximum value of the bottom (top) map is 0.123 G (1.49 G) and the minimum value of the bottom (top) map is −0.085 G (−1.09 G). Both maps are depicted to the same scale. It should be pointed out that these errors are very small compared with the maximum (minimum) value of $\nabla_2^2 B \times 0.5^2/2!$ which is 447 G (−948 G).

Numerical computation starts with the data of $B(x, y)$ stored in a uniform square mesh with $\Delta x = \Delta y = 0.1$. Data from $-4 \le x \le 4$ and $-4 \le y \le 4$ were chosen for comparison because this is the region where rapid change in the field values takes place. Field data expressed in kG up to the 11th decimal place were used to avoid the effects of truncation error. The values of the fourth (sixth) order term were obtained by applying the ∇_2^2 operator twice (three times).

The values listed in Table I show that for the second order term, the proposed CFD scheme is superior to the FD scheme by 14 times and superior to the scheme in Eq. (24) by 205 times. But as we move on to the higher order terms, the accuracy degrades because rapidly varying components of data become more and more dominant for higher order derivative terms.

5. APPLICATION TO THE MAGNETIC FIELD OF THE K1200 SUPERCONDUCTING CYCLOTRON

The K1200 superconducting cyclotron was built at the National Superconducting Cyclotron Laboratory to accelerate a variety of heavy ions for nuclear physics experiments and other applications. The median plane field map

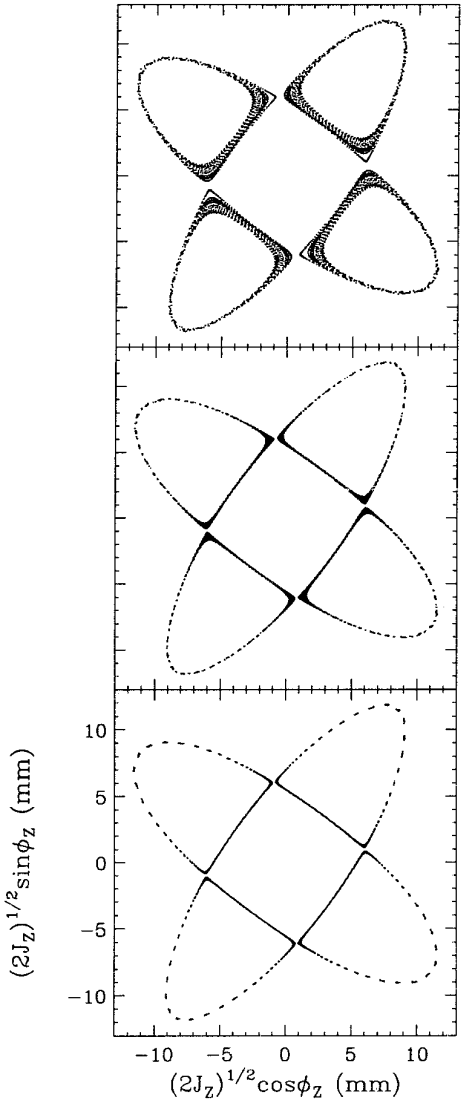

FIG. 7. Three maps of orbits at $\nu_z = 0.740$ near the $\nu_z = 3/4$ resonance obtained by plotting every 120° for 1000 turns. These maps were obtained by using three different versions of the Z^4 Orbit Code, which differ only in the numerical methods for computing derivatives: the code used for producing the top map makes use of Eq. (23) and Eq. (24) for computing field derivatives, the code for the middle map uses the finite difference differentiators [3], and the code for the bottom map utilizes the proposed compact finite difference differentiators. (J_z, ϕ_z) is the action-angle variable pair (see Fig. 8 also).

is measured in units of kG up to 5th decimal place in the polar mesh with $\Delta\theta = 1°$ and $\Delta r = 0.1$ in. while the radius of the machine is 42 in.

The magnetic field used as an example is for particles with charge per nucleon $q/A = 0.25$ and a nominal final energy per nucleon $E_f = 40$ MeV. For orbit computations, modified versions of the Z^4 Orbit Code [1] were used, which differ only in the numerical techniques for evaluating derivatives in Eqs. (1), (2), and (3). The results of orbit computation conducted at $\nu_z = 0.740$ near the $\nu_z = 3/4$ resonance are presented.

Three different results of orbit computation are presented in Fig. 7. These maps were obtained by plotting every 120° for 1000 turns. The map at the top was obtained by using Eqs. (23), (24) as differentiators, the map in the middle by using the finite difference schemes in [3], and the map at bottom by using the proposed compact finite difference schemes. In order to contrast the difference between the proposed CFD and the FD methods, magnified maps around the unstable fixed point in the first quadrant are presented in Fig. 8. The map at the top (bottom) in Fig. 8 is a magnification of the middle (bottom) map in Fig. 7. The more differentiators systematically underestimate the derivatives (see Figs. 3 and 5) of physically important slowly varying components of data, the more spiraling-in is observed. Even though the tracking code does not preserve symplectic conditions, these effects are shared by all the data because tracking codes use the same integrator. So the difference in each data is solely due to the differentiators used. That's why we concluded that

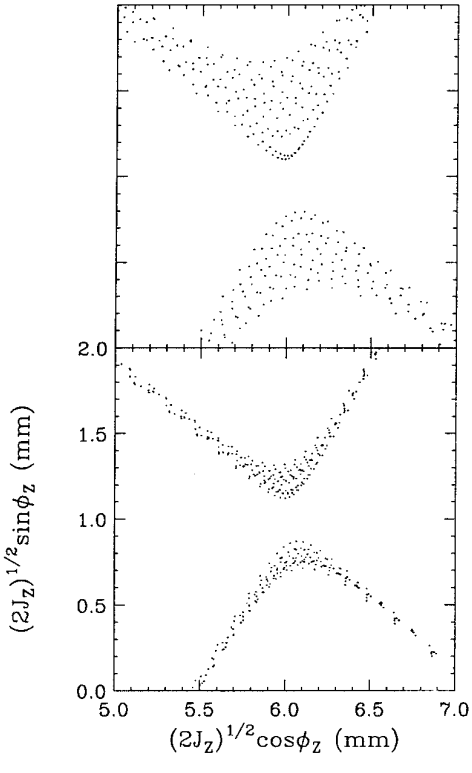

FIG. 8. Amplification of the middle and bottom maps in Fig. 7. The top (bottom) map is an amplification of the middle (bottom) map in Fig. 7 around the unstable fixed point in the first quadrant. The top map, obtained by using the finite difference differentiators [3], spirals in more than the bottom map, obtained by using the proposed compact finite difference differentiators by approximately three times.

systematic underestimation should be the cause. Although not presented in this paper, when we chose an orbit well inside the islands, we still observed similar spiraling-in (but the rate of spiraling-in was reduced). From the fact that the bottom map in Fig. 8 shows less inward spiraling than the top map by approximately three times, it could be concluded that the proposed compact finite difference method is indeed an improvement of the finite difference method presented in [3].

6. CONCLUSION

It has been shown that the proposed compact finite differentiators are better than the finite difference differentiators presented in [3] by comparing the low and high frequency response, by showing that the rms errors are considerably reduced when applied to a magnetic field where analytical expressions for field components are available, and by comparing the orbit tracking results when applied to measured magnetic field data of the K1200 superconducting cyclotron at the National Superconducting Cyclotron Laboratory at Michigan State University.

REFERENCES

1. M. M. Gordon and V. Taivassalo, *Nucl. Instr. Methods A* **247,** 423 (1986).
2. M. M. Gordon and V. Taivassalo, *IEEE Trans. Nucl. Sci.* **32,** 2447 (1985).
3. Dong-o Jeon, *J. Comput. Phys.* **117,** 55 (1995).
4. H. O. Kreiss, S. A. Orszag, and M. Israeli, *Annu. Rev. Fluid Mech.* ***6,*** 281 (1974).
5. R. S. Hirsch, *J. Comput. Phys.* **19,** 90 (1975).
6. Y. Adam, *J. Comput. Phys.* **24,** 10 (1977).
7. S. Lele, *J. Comput. Phys.* **103,** 16 (1992).
8. R. J. Thome and J. M. Tarrh, *MHD and Fusion Magnets* (Wiley, New York, 1982), p. 319.